Parametric Investigation Into the Effects of Pressure, Subcooling, Surface Augmentation and Choice of Coolant on Pool Boiling in the Design of Cooling Systems for High-Power-Density Electronic Chips

I. Mudawar
Director.

T. M. Anderson
Graduate Research Assistant.

Boiling and Two Phase Flow Laboratory,
School of Mechanical Engineering,
Purdue University,
West Lafayette, Ind. 47907

A high power electronic chip was simulated experimentally to investigate upper cooling capabilities using a variety of pool boiling enhancement techniques. Parametric effects of system pressure, subcooling, surface augmentation, and choice of coolant on boiling heat transfer from a vertical 12.7×12.7 mm² flat surface were examined. The two fluorocarbon coolants tested, FC-72 and FC-87, resulted in similar boiling curves, but FC-87 significantly reduced chip surface temperature for a given heat flux. Increasing pressure enhanced boiling performance and critical heat flux slightly. However, the significant increase in chip temperature, and the practical problems associated with packaging electronic hardware in a pressurized environment precluded pressurization as a viable enhancement option. Subcooling was very effective in increasing critical heat flux and significantly reducing bubble size and growth of the bubble boundary layer on the chip surface. Surface augmentation was also effective in enhancing critical heat flux; however, some surface geometries promoted noticeable temperature excursion at incipience.

1 Introduction

The quest for increased computational power has created a need for increasing signal speed in computer systems. This need has attracted worldwide research on speed enhancing technologies such as parallel processing, optical data transmission, galliumarsenide semiconductors and superconductivity. Presently, the two most popular techniques for speed enhancement are high-density packaging and increased voltage differentials. These approaches have led to increased energy dissipation at the chip, module, and system levels, with chip power densities projected to exceed 100 W/cm^2 by the mid-1990s (Bar-Cohen et al., 1986). The increased chip cooling needs have made obsolete many conventional air cooling techniques, and even some decade-old technologies such as indirect cooling by water.

During the last five years, many packaging engineers have shifted their attention to direct immersion cooling to reduce the overall thermal resistances of cooling hardware. The two direct immersion cooling options currently under consideration are single-phase and two-phase cooling.

Although relatively little work has been published on direct immersion two-phase electronic cooling using appropriate dielectric fluids, four areas of boiling are now under increasing examination: pool, channel flow, falling film, and jet impingement. Samant and Simon (1986) and Maddox and Mudawar (1989) examined forced convection boiling in a channel. Mudawar and Maddox (1989) demonstrated the capability of achieving very high flux values (>360 W/cm^2) with FC-72 by the combined use of subcooling and surface augmentation. Falling film cooling places less demands on pumping power but suffers from lower critical heat flux (CHF) values. Simulation of a gravity-assisted falling film apparatus suggested by Mudawar et al. (1987) proved the concept's freedom from boiling hysteresis, but showed CHF capability on the order of only 40 W/cm^2 for FC-72 (Grimley et al., 1988). Ma and Bergles (1983) attained in excess of 110 W/cm^2 with jet-impingement cooling using R-113. They noted, however, that the implementation of two-phase jet-impingement cooling may be complicated by interference between jets.

Contributed by the Electrical and Electronics Packaging Division for publication in the JOURNAL OF ELECTRONIC PACKAGING. Revised manuscript received by the Electrical and Electronics Packaging Division September 15, 1990.

Copyright © 1990 by ASME
Downloaded 29 Jul 2010 to 128.211.163.127. Redistribution subject to ASME license or copyright; see http://www.asme.org/terms/Terms_Use.cfm

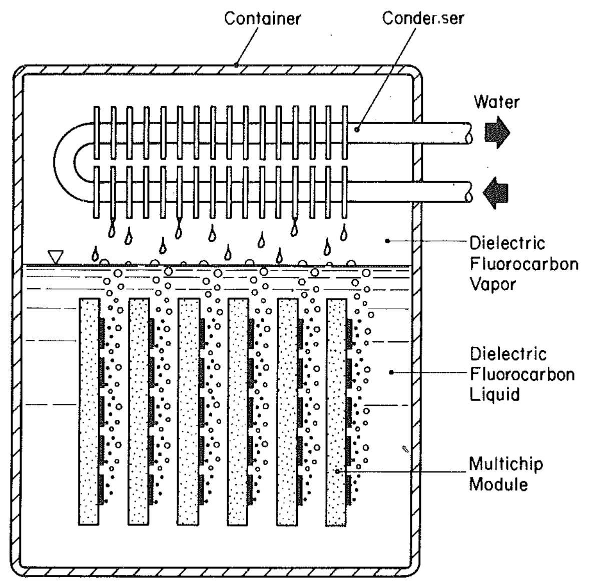

Fig. 1 Liquid encapsulated gravity-assisted thermosyphon cooling concept

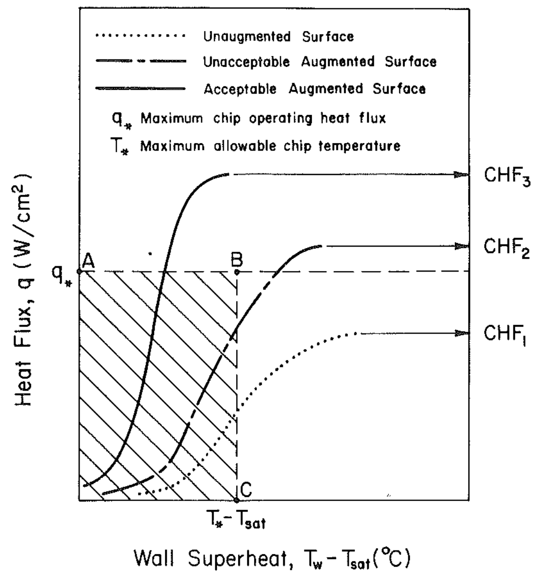

Fig. 2 Optimum boiling performance for electronic cooling

Enhanced pool boiling remains a prime candidate for the removal of large amounts of heat from multichip modules. Figure 1 shows a schematic of a typical pool boiling thermosyphon cooling system. This system possesses the benefits of passive fluid circulation, simplicity of construction, ease of sealing, and the absence of pump-induced fluid pulsation. Research on pool boiling in thermosyphon electronic cooling systems has been focused on three primary areas: (1) reducing the temperature excursion at incipient boiling, (2) reducing wall superheat during nucleate boiling, and (3) enhancing CHF. Achieving these objectives simultaneously remains a major challenge to the packaging engineer.

Surface enhancement is a very popular tool for improving pool boiling performance. Marto and Lepere (1982) found three commercially available enhanced boiling surfaces (Union Carbide High Flux, Hitachi Thermoexcel-E and Wieland Gewa-T) to significantly shift the boiling curve of FC-72 toward lower superheats compared to a plain copper surface. Anderson and Mudawar (1989) found microgroove and microstud surfaces to enhance CHF significantly compared to a plain surface, but at the expense of increased magnitude of incipience excursion. Nakayama et al. (1984) reported heat flux levels in excess of 110 W/cm^2 with a cylindrical fin constructed of stacked porous plates in FC-72.

Electronic cooling has to satisfy stringent requirements imposed by chip reliability criteria. Two parameters key to the choice of cooling configuration are the maximum heat flux generated at the chip surface, and the maximum allowable chip temperature (85°C for most mainframe memory and logic chips). Figure 2 explains the desired position of the boiling curve in relation to these two parameters. Curve 1 represents an unacceptable cooling performance because the chip exceeds the reliability-imposed temperature limit even at low power. The critical heat flux of the second curve (for an augmented surface) exceeds the maximum heat flux, but the enhancement of nucleate boiling is insufficient at keeping chip temperature below the allowable limit. Curve 3, on the other hand, is representative of an ideal cooling configuration capable of providing adequate heat removal within acceptable chip temperatures.

To achieve the desired cooling performance indicated by Curve 3 of Fig. 2, it is important to, simultaneously, increase CHF and reduce surface temperature. Increasing CHF in pool boiling can be achieved by: (1) increasing pressure, (2) sub-

Nomenclature

Bo = Bond number = $\dfrac{g(\rho_f-\rho_g)L^2}{\sigma}$
C_1 = empirical constant
c_p = specific heat at constant pressure
C_{sub} = subcooling constant
g = gravitational acceleration
Gr = Grashof number = $\dfrac{g\beta(\Delta T)L^3}{\nu^2}$
h = enthalpy
h_{fg} = latent heat of vaporization
Ja = modified Jacob number = $\dfrac{\rho_f c_{p,f}\Delta T_{sub}}{\rho_g h_{fg}}$
k = thermal conductivity
L = chip length (12.7 mm)
Nu = Nusselt number = $\dfrac{qL}{(\Delta T)k}$
Pr = Prandtl number
q = heat flux based on chip base area
q_m = critical heat flux (CHF)
$q_{m,z}$ = Zuber baseline CHF = $0.131\,\rho_g h_{fg}\left[\dfrac{g(\rho_f-\rho_g)\sigma}{\rho_g^2}\right]^{1/4}$
Ra = Rayleigh number = GrPr = $\dfrac{g\beta(\Delta T)L^3}{\nu\alpha}$
T = temperature
ΔT = $T_w - T_\infty$
ΔT_i = incipient wall superheat = $T_{w,i} - T_{sat}$
ΔT_{sat} = wall superheat = $T_w - T_{sat}$
ΔT_{sub} = degree of subcooling = $T_{sat} - T_\infty$
U = characteristic velocity
We = Weber number = $\dfrac{\rho_f U^2 L}{\sigma}$
α = thermal diffusivity
β = expansion coefficient
λ_T = Taylor wavelength = $2\pi\left[\dfrac{\sigma}{(\rho_f-\rho_g)g}\right]^{1/2}$
μ = dynamic viscosity
ν = kinematic viscosity
ρ = density
σ = surface tension

Subscripts

f = liquid
g = vapor
i = incipience
m = maximum (CHF)
sat = saturated
sub = subcooled
w = wall
∞ = bulk liquid
85 = 85°C chip temperature limit

Downloaded 29 Jul 2010 to 128.211.163.127. Redistribution subject to ASME license or copyright; see http://www.asme.org/terms/Terms_Use.cfm

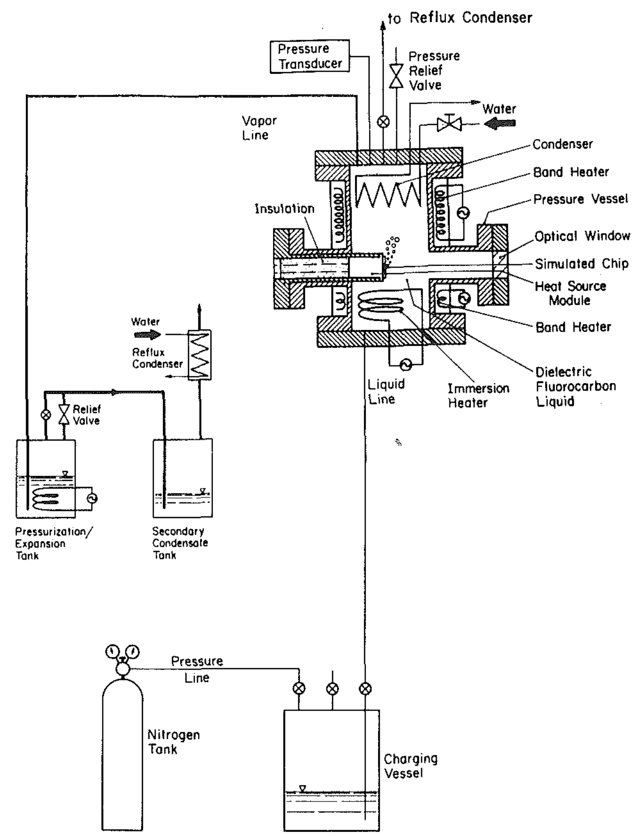

Fig. 3 Schematic diagram of experimental facility

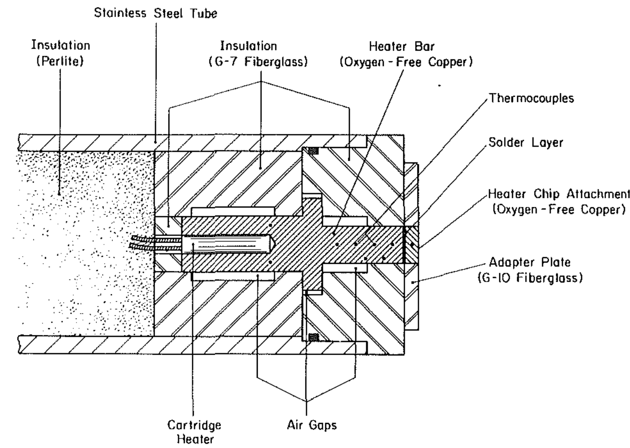

Fig. 4 Sectional diagram of test heater

cooling, and (3) surface enhancement. Reducing chip surface temperature, on the other hand, requires: (1) subcooling, (2) surface enhancement, or (3) the use of a dielectric coolant with a lower boiling point. The purpose of this study is to determine the parametric influences of these boiling augmentation techniques for smooth and enhanced chip attachments built upon a 12.7×12.7 mm^2 vertical surface.

2 Experimental Methods

Experimental Facility. The experimental facility consisted of a containment vessel designed and instrumented for the purpose of simulating pool boiling in a microelectronic cooling environment. As shown in Fig. 3, the main components of the facility were the vessel itself, external charging and subcooling tanks, and instrumentation and control systems. The vessel had an inner diameter of 202.7 mm and an inner height of 406.4 mm. Temperature control of the working fluid in the test vessel was achieved by means of an internal immersion heater, external band heaters, internal condenser, and an external reflux condenser. For subcooled experiments, the pressure vessel was filled with liquid and an external pressure control subsystem was needed to control pressure and temperature of the test fluid independently.

A high thermal capacitance heat source was chosen for this study to withstand numerous high temperature excursions that accompany CHF without physical burnout. The design of the heat source was similar to that used by Nakayama et al. (1984) and Park and Bergles (1986). As shown in Fig. 4, a cartridge heater conducted thermal energy through a calorimeter section into the boiling surface. Heat flux through the test surface was determined by a linear curve fit to the temperature readings of four thermocouples inserted along the axis of the calorimeter section. Repeatability experiments proved the present boiling data were consistent within $\pm$ 0.1°C at heat flux levels below 1 W/cm^2 and $\pm$ 0.2°C for higher fluxes. Further details concerning accuracy and calibration of the heater measurements can be found in a previous paper by Anderson and Mudawar (1989).

All enhanced surface attachments were built upon a 4.78 mm-thick base chip with a surface area of 12.7×12.7 mm^2. The base chips of these attachments were soldered directly to the calorimeter section of the test heater. Each boiling surface was vapor blasted with an air/water/silica slurry prior to testing to control hysteresis and ensure uniform and predictable surface microstructure (Anderson and Mudawar, 1989).

Test Procedure. A standardized test procedure was devised to ensure consistency between experimental runs. For saturated boiling data, the test chamber was partially filled with liquid to a level above the upper edge of the chip. The immersion heater was energized to raise fluid temperature to the desired saturated condition. At the same time, the wall temperature of the vessel was increased by the band heaters to reduce heat loss from the fluid. After reaching saturated conditions, the fluid was deaerated by 30 minutes of vigorous boiling. The test heater was also energized during the same period to remove air trapped within chip surface cavities. A reflux condenser mounted above the vessel (not shown in Fig. 3) condensed fluorocarbon vapor as noncondensible gases escaped freely to the ambient. Following deaeration, power to the immersion heater was reduced to bring the fluid into a nonboiling mode at saturated conditions, and the test heater was turned off as the saturated conditions were being maintained by the hand heaters. After an 8-hour waiting period, the boiling data were generated by supplying power to the test heater in small increments, and recording steady-state readings following each increment. The test procedure was terminated at CHF when a rapid unsteady increase in chip temperature was detected following a small increase in chip power. This condition was also confirmed visually and photographically by the formation of a vapor blanket on the chip surface which signaled transition to film boiling.

The test procedure was modified in the subcooled experiments by the use of the pressure control subsystem shown in Fig. 3. The pressure vessel was completely filled with liquid and the immersion heater energized to elevate liquid temperature to saturated conditions at the desired operating pressure. The fluid was then deaerated by 30 minutes of vigorous boiling in the test vessel and pressurization tank. The test heater was also energized during this period to rid the chip surface of noncondensible gases. The secondary condensate tank collected fluorocarbon liquid returned by the reflux condenser as air escaped the system. Following deaeration, the condensate tank was isolated from the system, and the heaters within the

Downloaded 29 Jul 2010 to 128.211.163.127. Redistribution subject to ASME license or copyright; see http://www.asme.org/terms/Terms_Use.cfm

Table 1 Comparison of properties and dimensionless parameters of FC-72 and FC-87 at one atmosphere

Parameter	Symbol	Units	FC-72	FC-87	FC-72*/FC-87
Temperature	T	°C	56	30	—
Molecular weight	—	—	340	290	—
Liquid enthalpy	h_f	kJ/kg	59.80	32.04	—
Heat of vaporization	h_{fg}	kJ/kg	84.73	88.52	0.957
Vapor enthalpy	h_g	kJ/kg	144.53	120.56	—
Liquid density	ρ_f	kg/m^3	1620.94	1746.99	0.928
Vapor density	ρ_g	kg/m^3	13.01	12.78	1.018
Dynamic viscosity	μ_f	$10^6 kg/ms$	447.0	447.4	0.999
Kinematic viscosity	ν_f	$10^6 m^2/s$	0.2746	0.2600	1.056
Surface tension	σ	mN/m	9.48†	8.89	1.066
Specific heat	$c_{p,f}$	kJ/kg K	1.096	1.090	1.006
Thermal conductivity	k_f	$10^3 W/m\ K$	53.84	55.21	0.975
Thermal diffusivity	α_f	$10^6 m^2/s$	0.0303	0.0290	1.045
Expansion coefficient	β_f	$10^3 °C^{-1}$	1.64	1.57	1.044
Bond number††	Bo	—	166.39	191.37	0.868
Grashof number	Gr_f	—	—	—	0.936
Jacob number	Ja	—	—	—	0.957
Prandtl number	Pr_f	—	9.061	8.968	1.010
Rayleigh number	Ra_f	—	—	—	0.946
Weber number	We	—	—	—	0.955
Taylor wavelength	λ_T	mm	4.871	4.542	0.932
Zuber CHF	$q_{m,z}$	W/cm^2	14.01	14.39	0.963

*Ratios of dimensionless numbers are based on identical values of length, velocity, ΔT or ΔT_{sub}.
†Measured experimentally at Purdue's Boiling and Two-Phase Flow Laboratory using a Kruss K8 ring-type tensionmeter.
††Based on a 12.7 mm characteristic length.

pressurization tank were energized to maintain fluid temperature at a level corresponding to the desired operating pressure. Next, the water line of the condenser submerged in the test vessel was opened to subcool liquid in the vessel to the desired temperature. Boiling data were generated by following a procedure similar to that of the saturated tests.

3 Experimental Results

Effect of Coolant Properties. The Fluorinert series of electronic liquids (FC-40, −43, −71, −72, −74, −75, −77, −84, −86, and −87) manufactured by 3M are widely accepted in the electronics industry for such applications as chip testing, direct immersion cooling, and condensation soldering (3M Fluorinert Electronic Liquids Product Manual, 1988). Containing no hydrogen or chlorine, these clear odorless carbon/fluorine fluids are believed to pose no threats to the ozone layer. They are also extremely inert and stable, non-flammable and non-reactive, and are available in a 30° to 174°C range of boiling points at atmospheric pressure. They maintain low viscosities down to freezing points less than −50°C. While compatible with most electronic hardware materials, the Fluorinerts unfortunately possess an unusually high air solubility (up to 50 percent by volume; Kraus and Bar-Cohen, 1983) which may result in boiling incipience temperatures well below the saturation temperature of the pure fluid (Murphy and Bergles, 1971). Thus, the use of Fluorinerts for electronic cooling requires careful deaeration to ensure predictable cooling performance.

The two fluids most commonly used for electronic cooling are FC-72 and FC-77 with atmospheric pressure boiling points of 56 and 97°C, respectively. Since the chip temperature has to be maintained below 85°C, FC-77 is ideal for single-phase cooling, while FC-72 is recommended for cooling systems involving phase change.

One drawback to the use of FC-72 is that its saturation temperature may be too high for electronic cooling involving heavily finned surfaces. These surfaces tend to increase CHF significantly at the expense of increasing chip surface temperature beyond 85°C, rendering CHF enhancement ineffective for electronic cooling. Thus, higher chip fluxes may require subcooling FC-72 or using a different coolant with a lower saturation temperature. One such fluid is Fluorinert FC-87 which has a saturation temperature of 30°C.

Table 1 shows the properties of FC-72 and FC-87 at one atmosphere along with some ratios of applicable dimensionless numbers and boiling parameters. These properties were obtained from the 3M Fluorinert Electronic Liquids Product Manual (1988) except for the viscosity values, which were obtained through a private communication with 3M personnel, and the FC-72 surface tension data which were measured by the authors at the Purdue University Boiling and Two-Phase Flow Laboratory. Comparing the fluid properties shows strong similarities between the fluids despite differences in their boiling points. Examination of the Rayleigh number ratio, bond number and Zuber baseline CHF (Zuber, 1958) indicates FC-72 and FC-87 should have very similar boiling curves.

Figure 5 also shows important facts concerning the useful operating temperature ranges of the two fluids. By examining of the Bond number, the ratio of gravitational to surface tension forces, it may be possible to draw qualitative conclusions concerning nucleate boiling performance in comparing the two fluids. The ratio of $Bo_{72}/Bo_{87} = 0.869$ is manifested in Fig. 5 by a slight leftward shift of the FC-87 boiling curve to lower wall superheat. Furthermore, boiling commences in FC-87 at

Downloaded 29 Jul 2010 to 128.211.163.127. Redistribution subject to ASME license or copyright; see http://www.asme.org/terms/Terms_Use.cfm

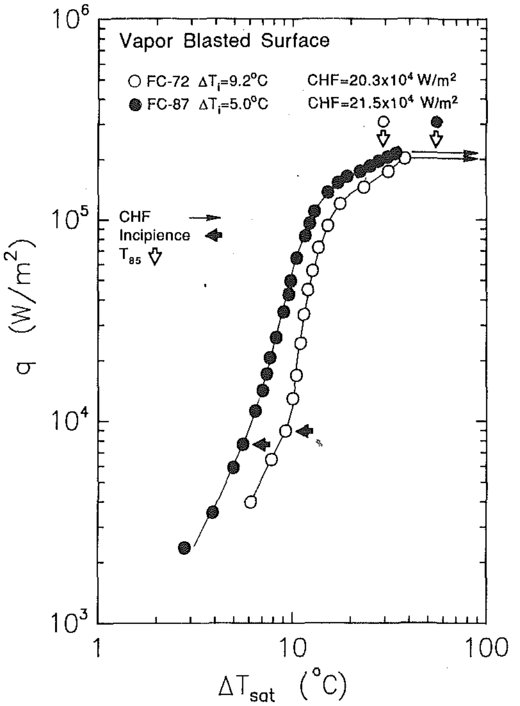

Fig. 5 Effect of fluid variation on the boiling performance of a flat surface

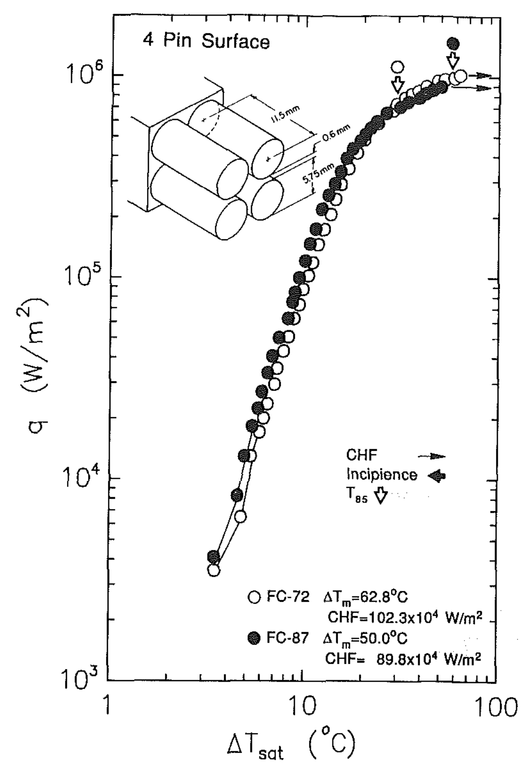

Fig. 6 Effect of fluid variation on the boiling performance of a 4 pin surface

35°C and reaches CHF at 64°C, 21° below the 85°C maximum chip temperature guideline; while FC-72 reaches CHF beyond the 85°C limit. Thus, it is evident that FC-87 outperforms FC-72 in maintaining lower chip temperatures.

Figure 6 displays data for boiling of FC-72 and FC-87 from a heavily finned surface. The CHF values of the enhanced geometry ($q_{m,72}$ = 102 W/cm², $q_{m,87}$ = 89.8 W/cm²) represent fivefold increases in critical heat flux over the flat surface. However, the base temperature for the 4 pin surfaces in FC-87 increased at CHF to 80°C, still below the 85°C guideline, while CHF in FC-72 occurred at a chip temperature 30° over the acceptable limit. This indicates that, although FC-87 may not always be necessary for cooling plain chips, it may provide performances far superior to FC-72 with high-profile surface augmentation.

Table 2 Saturation temperatures and pressures of FC-72 and FC-87

Fluid	Pressure (atm)	Temperature (°C)
FC-72	1	56
	2	78
	3	93
	4	104
	5	112
FC-87	1	30
	2	50
	3	63
	4	74
	5	82

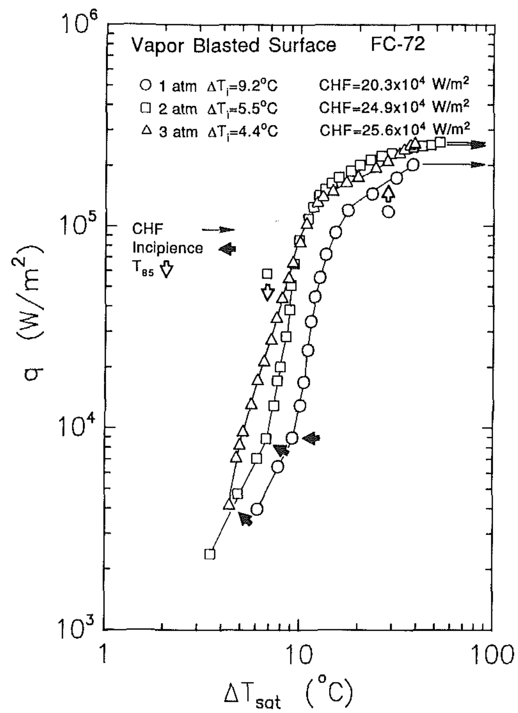

Fig. 7 Effect of pressurization on boiling of FC-72 on a flat surface

Pressure Effect. Another means of increasing CHF is to operate at an elevated pressure. However, temperature and strength consideration associated with the chips and the containment vessel preclude cooling at very high pressures. Table 2 shows the saturation temperatures and pressures for FC-72 and FC-87 over a 1 to 5 atmosphere pressure range. Based on an 85°C chip temperature limit, FC-72 and FC-87 must be held below 3 and 6 atmospheres, respectively, based on the saturation temperature of the fluid alone.

A flat vapor blasted surface was tested at 1, 2, and 3 atmospheres in FC-72 to examine trends in the boiling curve dependence on saturation pressure. Figure 7 shows increases in the nucleate boiling heat transfer coefficient and critical heat flux with increased pressure, concurrent with the expected trend of increasing chip surface temperature, with CHF occurring above 85°C for the three pressures. Thus, only FC-87

Downloaded 29 Jul 2010 to 128.211.163.127. Redistribution subject to ASME license or copyright; see http://www.asme.org/terms/Terms_Use.cfm

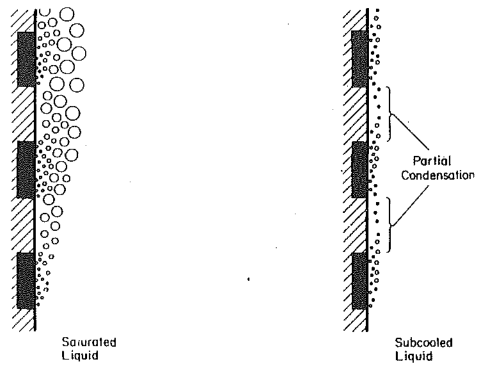

Fig. 8 Development of a bubble boundary layer on a multichip array

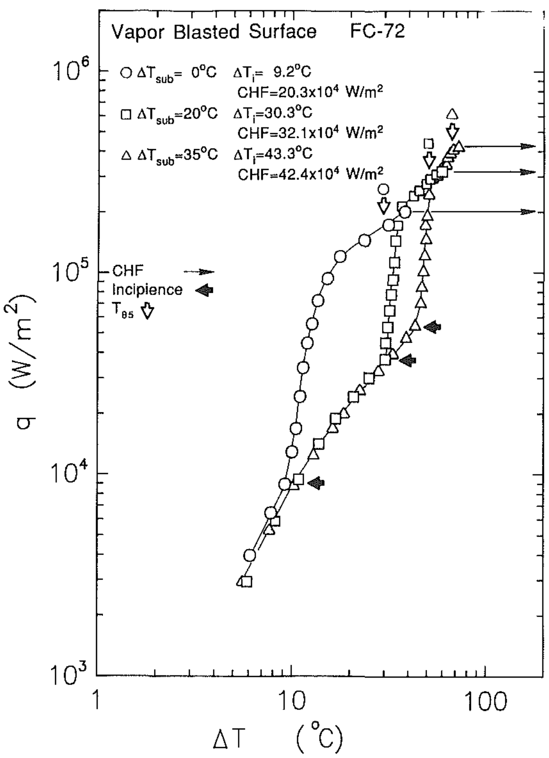

Fig. 9 Effect of subcooling on boiling of FC-72 on a flat surface

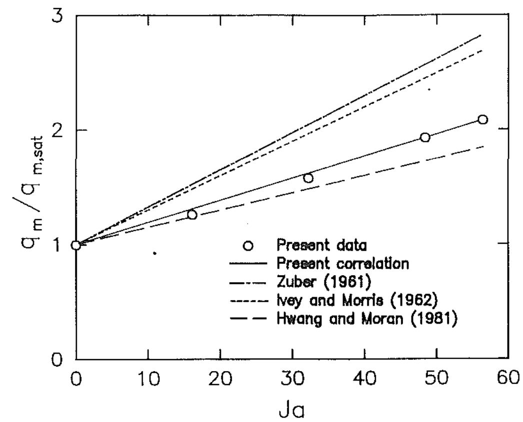

Fig. 10 Correlation of present subcooled FC-72 CHF data along with those of other investigators

Table 3 Correlation constants for subcooled CHF

Author	C_{sub} ($°C^{-1}$)	C_1
Zuber (1961)	0.0522	–
Ivey and Morris (1962)	0.0482	0.1
Hwang and Moran (1981)	0.0241	0.05
Present study	0.0310	0.0643

would make use of the marginal increase in CHF with increasing pressure.

Considering the insignificant enhancement in CHF, the sharp increase in chip temperature, and the practical problems associated with electronic packaging in a pressurized environment, it may be concluded that pressurization is not a viable enhancement option for electronic cooling.

Subcooling Effect. Subcooling offers many advantages over saturated boiling for cooling large arrays of computer chips due to the decreased diameter and rapid collapse of departing bubbles. Figure 8 shows how the thickness of the bubble boundary layer in saturated liquid grows significantly in the direction of buoyancy-induced bubble flow. Hence, the upper chips experience less favorable boiling conditions (greater void fraction and higher wall superheat) than lower chips.

Figure 9 shows data taken with FC-72 on a flat vapor blasted surface with $\Delta T_{sub} = 0°, 20°$ and $35°C$ at atmospheric pressure. These boiling curves display significant increases in the incipient and critical heat fluxes with increasing degree of subcooling. However, the surface temperatures corresponding to incipience and CHF remained within 2° bandwidths over the 35°C subcooling range.

Subcooled pool boiling CHF data are commonly correlated with a linear dependence on the degree of subcooling,

$$\frac{q_m}{q_{m,\,sat}} = 1 + C_{sub}\,\Delta T_{sub} \quad (1)$$

where $q_{m,\,sat}$ is the CHF value for saturated boiling and C_{sub} is a semi-empirically determined subcooling augmentation factor. Zuber et al. (1961) recommended the relation

$$C_{sub} = 5.3\,\frac{\sqrt{k_f\,\rho_f\,c_{p,\,f}}}{\rho_g h_{fg}}\left[\frac{g\sigma(\rho_f-\rho_g)}{\rho_g^2}\right]^{1/8}\left[\frac{g(\rho_f-\rho_g)}{\sigma}\right]^{1/4} \quad (2)$$

which agreed with data for water and ethyl alcohol at pressures below approximately 5 bar. Ivey and Morris (1962) suggested a simpler form for C_{sub},

$$C_{sub} = C_1\,\frac{\rho_f\,c_{p,\,f}}{\rho_g h_{fg}}\left(\frac{\rho_g}{\rho_f}\right)^{1/4} \quad (3)$$

which was successful in correlating data for many fluids over a wide pressure range using the empirical constant $C_1 = 0.1$. Hwang and Moran (1981) tested equation (3) against their data for FC-72 boiling on a vertical 4.57 mm square silicon chip at atmospheric pressure and determined a much lower value of $C_1 = 0.05$. They attributed the decrease in CHF augmentation with subcooling compared to equation (3) to the vertical orientation of their chip, postulating that the thermal boundary layer on the chip and surrounding substrate was impeding free access of the cooler bulk liquid to the chip.

Combining equations (1) and (3) yields

$$\frac{q_m}{q_{m,\,sat}} = 1 + C_1\left(\frac{\rho_g}{\rho_f}\right)^{1/4}\frac{\rho_f\,c_{p,\,f}\,\Delta T_{sub}}{\rho_g h_{fg}} = 1 + C_1\left(\frac{\rho_g}{\rho_f}\right)^{1/4}\text{Ja} \quad (4)$$

where Ja is the modified Jacob number. Figure 10 shows CHF data obtained at 0, 10, 20, 30 and 35°C along with the pre-

Downloaded 29 Jul 2010 to 128.211.163.127. Redistribution subject to ASME license or copyright; see http://www.asme.org/terms/Terms_Use.cfm

Table 4 Subcooled FC-72 CHF data at one atmosphere

ΔT_{sub} °C	CHF × 10^{-4} (W/m²)	T_m (°C)
0	20.3	94.1
10	25.7	91.5
20	32.1	95.3
30	39.2	97.5
35	42.3	93.2

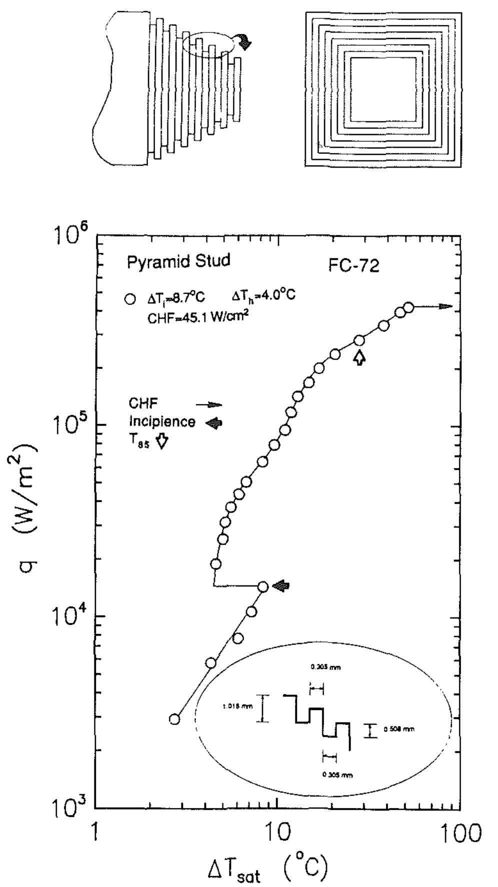

Fig. 11 Saturated boiling of FC-72 on the pyramid stud

viously mentioned correlations. The empirical constant C_1 = 0.064 correlates the present data with a mean absolute deviation of 1.4 percent with all points falling within 3.5 percent of the correlation. Table 3 shows the coefficients for the subcooled CHF correlations using the properties of FC-72 at atmospheric pressure. Both the present data and those of Hwang and Moran (1981) display significant departure from the correlations of Zuber et al. (1961) and Ivey and Morris (1962) developed earlier for boiling on a horizontal surface.

Table 4 shows a 35°C subcooling increased CHF by a factor of 2.08 compared to saturated boiling, while maintaining a fairly constant wall temperature at CHF. The increased CHF, coupled by a reduction in the growth of the bubble boundary layer in a subcooled liquid, suggests subcooling is a very effective means of enhancing CHF for a vertical array of chips as illustrated in Fig. 8.

Unless the two-phase cooling system is modified with a secondary refrigeration unit, the lower practical temperature of water circulated in the condenser would be limited to approximately 10°C, placing upper limits on the degree of subcooling of 46 and 20°C for FC-72 and FC-87, respectively. Thus, the enhancement potential of subcooling is greater for FC-72 than for FC-87.

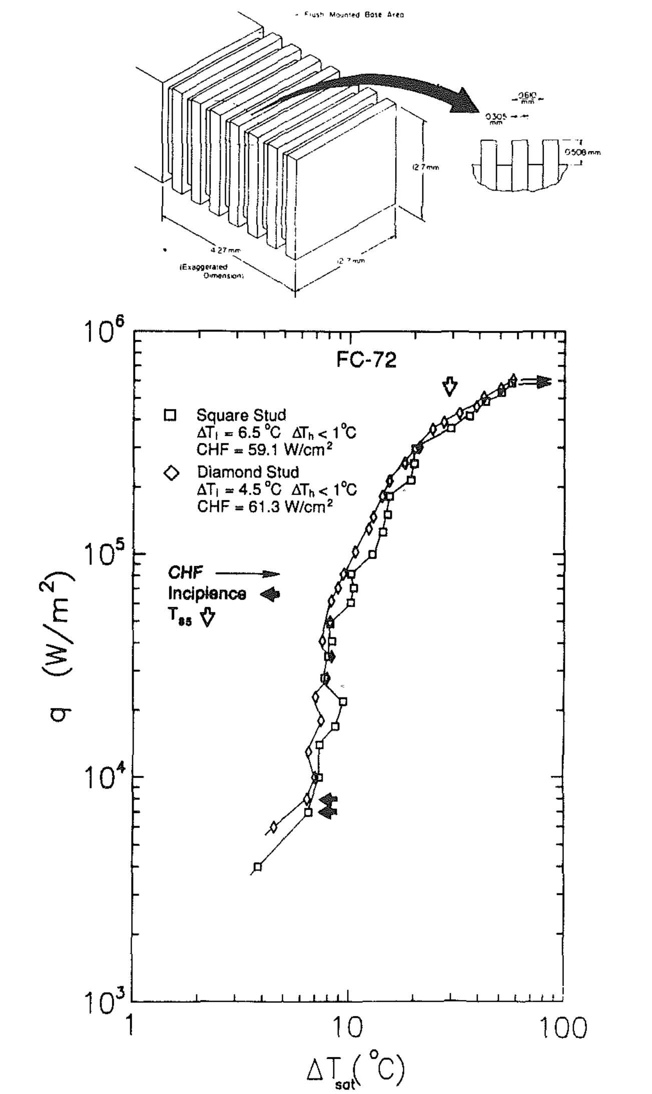

Fig. 12 Saturated boiling of FC-72 on the square stud in two orientations

Effect of Enhanced Surface Shape and Geometry. Anderson and Mudawar (1989) performed a parametric investigation into the effects of surface structure on the temperature excursion associated with incipience. They demonstrated that microstructures (microgrooves or microstuds) machined into chip attachments enhance nucleate boiling and CHF while increasing the magnitude of the incipience excursion.

In an attempt to capitalize on the advantages of surface microstructures while reducing the incipience excursion, a pyramid geometry with an extended profile was fabricated with microgrooves around its perimeter similar to those used by Anderson and Mudawar (1989). The pyramid stud was 4.27 mm long and its four sides were inclined 39.8 degrees with respect to the axis. It was believed that the relatively large thermal mass of the pyramid would dampen the excursion. Figure 11 shows a 4°C temperature drop caused by an unexpected pattern of nucleate boiling activation. Boiling was initiated near the base of the underside of the pyramid. From this position, bubbles would escape following two paths: (1) circumferentially within the microgroove, from the underside towards the two vertical sides, and (2) across microgrooves obliquely along the underside towards the tip and continuing upwards over the tip surface. The bubbles traveling the latter path helped activate boiling over the entire underside of the pyramid which, in turn, triggered boiling everywhere on the pyramid, resulting in a noticeable excursion.

Downloaded 29 Jul 2010 to 128.211.163.127. Redistribution subject to ASME license or copyright; see http://www.asme.org/terms/Terms_Use.cfm

Figure 12 shows data obtained previously by Anderson and Mudawar (1989) using a square-shaped stud with microgrooves machined into its perimeter. The stud was tested in "square" and "diamond" configurations with the stud axis maintained in a horizontal plane for both configurations. The "diamond" configuration was achieved by rotating the heater module 45 degrees about its axis, placing all chip sides in oblique orientation with respect to gravity. Unlike the pyramid geometry, the untapered shape of the square stud was believed to restrain bubble motion toward the tip and, consequently, suppress activation of a large percentage of the heat transfer area. However, the square stud displayed a segmented curve in the "square" configuration, caused by a step-wise activation of boiling over its perimeter. Nucleation was initiated within a microgroove at the root of one vertical face of the stud. Increasing heat flux led to activation of a large portion of that face. Upon further increasing heat flux, activation migrated to the bottom face, other vertical face, and the upper face. The face was noticed to promote accumulation of bubbles beneath the stud, resulting in rapid activation of that lower face. The resultant relatively large step-wise increases in activation area created an unusual segmented boiling curve as shown in Fig. 12. On the other hand, the more streamlined buoyancy-induced bubble flow associated with the "diamond" configuration suppressed the nucleation front in a given microgroove from advancing freely into the neighboring microgroove, resulting in a gradual nucleation process and smoother boiling curve.

Based on the results shown in Figs. 11 and 12, it was determined that extended surface geometries be designed to inhibit activation of a large fraction of the surface area with a small increase in heat flux. Tapered or conical shapes, and shapes which promote accumulation of vapor bubbles are especially prone to the unstable activation pattern. Thus, it may be concluded that high-profile enhancement should be restricted to cylindrical shapes which are, fortunately, the most desirable from a fabrication standpoint. This type of enhancement is reminiscent of the work by Nakayama et al. (1984) who studied various enhancement geometries built onto extended cylindrical studs.

The authors have examined several cylindrical geometries including surfaces with a single pin, 4 pins and 9 pins, and microgroove and microstud enhancement built upon a single pin. Each of these surfaces displayed a gradual propagation of nucleation front with increased heat flux, and negligible excursion at incipience. As expected, all these surfaces increased CHF considerably over the flat surface due to the increased surface area, reaching fluxes in excess of 100 W/cm^2 in saturated FC-72 as shown in Fig. 6 for the 4 pin surface.

4 Summary

This study involved an examination of various techniques aimed at the enhancement of pool boiling performance from high power microelectronic chips. Specific findings from the study are as follows:

1. The enhancement benefits of extended surfaces in saturated FC-72 are outweighed by an increase in chip temperature above the maximum allowable guideline of 85°C. The lower boiling point of FC-87 makes this latter fluid an ideal coolant for heavily finned surfaces in saturated pool boiling.

2. Increasing pressure enhances boiling performance and CHF slightly while significantly increasing chip temperature. The sharp increase in temperature, coupled with a host of practical problems associated with packaging electronic hardware in a pressurized environment, precludes pressurization as a viable enhancement option.

3. Subcooling is a very powerful means of increasing CHF. Additionally, the reduced bubble size and controlled growth of the bubble boundary layer on the chip surface renders subcooling an essential means of ensuring uniform cooling for a multitude of chips mounted onto a single module.

4. Surface augmentation is effective at increasing critical heat flux; however, some surface geometries promote noticeable temperature excursion at incipience. Tapered or conical shapes, and shapes which promote accumulation of vapor bubbles are especially prone to unsteady propagation of the nucleation front. Cylindrical extended surfaces, on the other hand, combine the advantages of suppressing nucleation excursion with ease of fabrication. These cylindrical enhanced surfaces reached fluxes in excess of 100 W/cm^2 in saturated FC-72.

Acknowledgment

Support for this research by the IBM Corporation is gratefully acknowledged. The authors also appreciate receiving FC-72 and FC-87 fluid samples from the Industrial Chemical Products Division of 3M.

References

Anderson, T. M., and Mudawar, I., 1989, "Microelectronic Cooling by Enhanced Pool Boiling of a Dielectric Fluorocarbon Liquid," ASME *Journal of Heat Transfer*, Vol. 111, pp. 752–759.

Bar-Cohen, A., Mudawar, I., and Whalen, B., 1986, "Future Challenges for Electronic Cooling," *Research Needs in Electronic Cooling*, F. P. Incropera, ed., published by the National Science Foundation and Purdue University, pp. 70–77.

Fluorinert Electronic Liquids Product Manual, 1988, 3M Industrial Chemical Products Division, 3M Center, St. Paul, Minnesota.

Grimley, T. G., Mudawar, I., and Incropera, F. P., 1988, "Limits to Critical Heat Flux Enhancement in a Liquid Film Falling over a Structured Surface which Simulates a Microelectronic Chip," ASME *Journal of Heat Transfer*, Vol. 110, pp. 535–538.

Hwang, U. P., and Moran, K. P., 1981, "Boiling Heat Transfer of Silicon Integrated Circuits Chip Mounted on a Substrate," *Heat Transfer in Electronic Equipment*, HTD-Vol. 20, M. D. Kelleher and M. M. Yovanovich, eds., ASME, pp. 53–59.

Ivey, H. J., and Morris, D. J., 1962, "On the Relevance of the Vapor-Liquid Exchange Mechanism for Subcooled Boiling Heat Transfer at High Pressure," Rept. AEEW-R137, United Kingdom Atomic Energy Authority, Winfrith, England.

Kraus, A. D., and Bar-Cohen, A., 1983, *Thermal Analysis and Control of Electronic Equipment*, McGraw-Hill, New York, p. 190.

Ma, C. F., and Bergles, A. E., 1983, "Boiling Jet Impingement Cooling of Simulated Microelectronic Chips," *Heat Transfer in Electronic Equipment*, HTD-Vol. 28, ASME, pp. 5–12.

Maddox, D. E., and Mudawar, I., 1989, "Single and Two-Phase Convective Heat Transfer from Smooth and Enhanced Mircoelectronic Heat Sources in a Rectangular Channel," ASME *Journal of Heat Transfer*, Vol. 111, pp. 1045–1052.

Marto, P. J. and Lepere, V. J., 1982, "Pool Boiling Heat Transfer from Enhanced Surfaces to Dietectric Fluids," ASME *Journal of Heat Transfer*, Vol. 104, pp. 292–299.

Mudawar, I. A., Incropera, T. A., and Incropera, F. P., 1987, "Microelectronic Cooling by Fluorocarbon Liquid Films," *Proc. Int. Symp. on Cooling Technology for Electronic Equipment*, Honolulu, Hawaii, Mar., pp. 340–357.

Mudawar, I., and Maddox, D. E., 1989, "Enhancement of Critical Heat Flux from High Power Microelectronic Heat Sources in a Flow Channel," *Heat Transfer in Electronics*, HTD-Vol. 111, ASME, R. K. Shah, ed., pp. 51–58.

Murphy, R. W., and Bergles, A. E., 1971, "Subcooled Flow Boiling of Fluorocarbons," MIT Heat Transfer Laboratory and Engineering Projects Laboratory Report 71903-72, Cambridge, Mass.

Nakayama, W., Nakajima, T., and Hirasawa, S., 1984, "Heat Sink Studs having Enhanced Boiling Surfaces for Cooling of Microelectronic Components," ASME Paper 84-WA/HT-89.

Park, K. A., and Bergles, A. E., 1986, "Boiling Heat Transfer Characteristics of Simulated Microelectronic Chips with Detachable Heat Sinks," *Proc. 8th Int. Heat Transfer Conf.*, San Francisco, Calif., Vol. 4, pp. 2099–2104.

Samant, K. R., and Simon, T. W., 1986, "Heat Transfer from a Small, High-Heat-Flux Patch to a Subcooled Turbulent Flow," ASME Paper 86-HT-22.

Zuber, N., Tribus, M., and Westwater, J. W., 1961, "The Hydrodynamic Crisis in Pool Boiling of Saturated and Subcooled Liquids," *Int. Developments in Heat Transfer*, Part 2, ASME, pp. 230–236.

Zuber, N., 1958, "Hydrodynamic Aspects of Boiling Heat Transfer," Rept. AECU-4439.

Downloaded 29 Jul 2010 to 128.211.163.127. Redistribution subject to ASME license or copyright; see http://www.asme.org/terms/Terms_Use.cfm